

Evidence for s_{\pm} -wave pairing symmetry in LiFeAs from its low-temperature specific heat

Dong-Jin Jang,¹ J. B. Hong,¹ Y. S. Kwon,^{1,2} and T. Park^{1,*}

¹*Department of Physics, Sungkyunkwan University, Suwon 440-746, Republic of Korea*

²*Department of Emerging Materials Science, Daegu Gyeongbuk Institute of Science and Technology, Daegu 711-873, Republic of Korea*

K. Gofryk, F. Ronning, and J. D. Thompson

Los Alamos National Laboratory, Los Alamos, New Mexico 87545, USA

Yunkyu Bang[†]

Department of Physics, Chonnam National University, Kwangju 500-757, Republic of Korea

(Received 11 February 2012; revised manuscript received 20 March 2012; published 18 May 2012)

We report specific heat capacity measurements on a LiFeAs single crystal at temperatures down to 400 mK and magnetic fields up to 9 T. A small specific heat jump at T_c and finite residual density of states at $T = 0$ K in the superconducting (SC) state indicate that there are strong unitary scatterers that lead to states within the SC gap. A sublinear magnetic field dependence of the Sommerfeld coefficient $\gamma(H)$ at $T = 0$ K is equally well fitted by both a nodal d -wave gap as well as a sign changing multiband s_{\pm} -wave gap. When impurity effects are taken into account, however, the linear temperature dependence of the electronic specific heat C_{el}/T at low temperatures argues against a nodal d -wave superconducting gap. We conclude that the SC state of LiFeAs is most compatible with the multiband s_{\pm} -wave SC state with the gap values $\Delta_{small} = 0.46\Delta_{large}$.

DOI: [10.1103/PhysRevB.85.180505](https://doi.org/10.1103/PhysRevB.85.180505)

PACS number(s): 74.70.Xa, 74.25.Bt, 74.20.Rp

Information on the superconducting (SC) pairing symmetry is important for the understanding of the SC pairing mechanism. For the newly discovered Fe-pnictide superconductors, determination of the SC order parameter has been controversial partly due to its sensitive dependence on measurement probes and material stoichiometry.^{1–4} It has been suggested that the sensitivity of the SC gap symmetry is related to the nearly compensated multiple bands at the Fermi surface that are susceptible to small changes in the doping or electronic structure.^{5,6} Additionally, the momentum space structure of the superconducting gap may be different at a physical surface than in the bulk.⁷ Therefore, measurements that mainly probe the surface may detect a nodeless gap, while bulk measurements may report a nodal gap, implying that it is important to consider both surface and bulk sensitive measurements for the determination of the SC gap symmetry in the Fe-pnictide superconductors.

LiFeAs, the so-called “111” phase, is unique in that it is superconducting without carrier doping and the residual resistivity ratio (RRR) is about 50, one of the highest among Fe-based SC compounds,⁸ holding promise for a determination of the superconducting gap symmetry without complications from material defects.^{9–13} Even though various theoretical and experimental studies point toward an isotropic SC gap without nodes on the Fermi surface,^{14–22} to the best of our knowledge, the nature of the order parameter symmetry has yet to be determined. Previous specific heat measurements, a direct bulk probe of the electronic density of states (DOS), suggest multiple SC gaps to explain its temperature dependence.^{22,23} The analysis, however, is limited due to a lack of specific heat data below 2 K in high quality samples, where a difference in the DOS becomes prominent among different types of SC pairing symmetries. In order to elucidate the nature of the order parameter of LiFeAs, we measured the specific heat of LiFeAs single crystals down to 400 mK and under magnetic fields up to 9 T. A large value of the Sommerfeld coefficient γ_0

(≈ 7.5 mJ/mol K²) in the SC state at zero magnetic field and a small specific heat jump ratio $\Delta C/C_n$ at T_c (≈ 0.5) indicates the presence of large elastic scattering due to impurities. Here C_n is the specific heat at T_c in the normal state. When the impurity effects are taken into account, observation of a linear temperature dependence of the low- T specific heat C/T and a sublinear magnetic field dependence of the Sommerfeld coefficient $\gamma(H)$ excludes a d -wave SC gap, but is consistent with the sign changing multiband s_{\pm} -wave state with the gap values $\Delta_{small} = 0.46\Delta_{large}$.

Single crystalline LiFeAs, which is formed in a $P4/nmm$ tetragonal Cu_2Sb -type structure with $a = 3.7818$ Å and $c = 6.3463$ Å, was synthesized in a sealed tungsten crucible by the Bridgman method.⁸ X-ray diffraction pattern analysis showed that crystals from this batch are homogeneous and well oriented. This growth technique seems to avoid inclusion of impurities that can lead to an anomalous Schottky-like upturn in the low-temperature specific heat of Fe-based superconductors, making it a useful synthesis technique for a specific heat study of SC gap symmetry.²⁴ The crystals used in the current study are from the same batch that has been used for previous transport and thermodynamic studies.^{8,15,16} A Quantum Design Physical Properties Measurement System (PPMS) with a ³He option was used to measure specific heat down to 400 mK and up to 9 T. For a magnetic field perpendicular to the tetragonal c axis, vertical placement of the platelike LiFeAs single crystal was done by eye on the sample holder, while the flat face of the crystal was placed parallel with the sample holder for H parallel to the c axis.

Figure 1(a) shows the temperature-dependent specific heat capacity of a LiFeAs single crystal at zero field. The superconducting transition temperature 15 K ($=T_c$), which is determined from the midpoint of the the specific heat anomaly, is lower than that determined from the electrical resistivity,⁸ possibly due to filamentary superconductivity. The measured specific heat (C) consists of electronic (C_{el}) and phononic

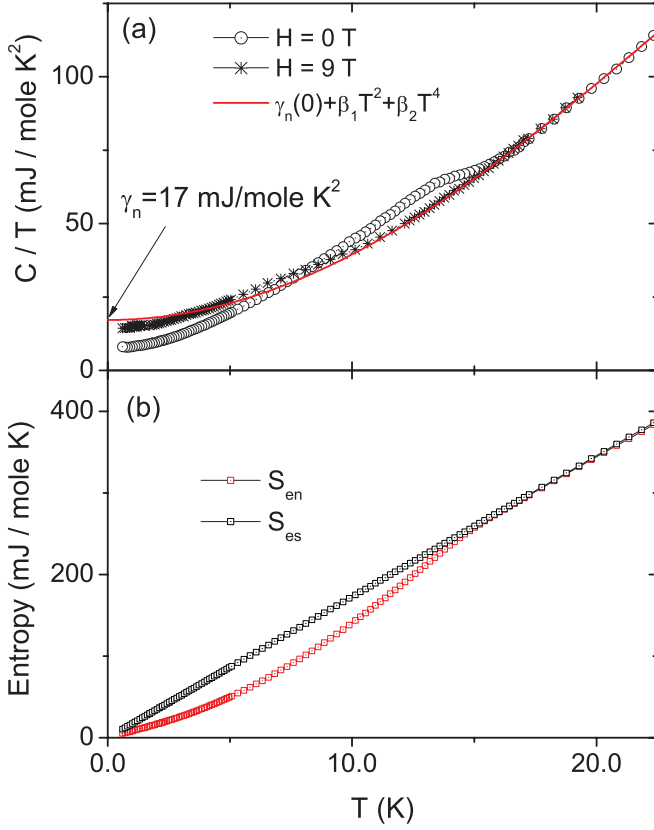


FIG. 1. (Color online) (a) Specific heat of LiFeAs is plotted at zero (open circles) and 9 T (stars) for a field parallel to the c axis. The red solid line is an estimated normal state specific heat C_n/T from a polynomial form described in the text. (b) Calculated electronic entropy in the superconducting state (S_{es}) and in the normal state S_{en} .

(C_{ph}) contributions, i.e., $C = C_{el} + C_{ph}$. Non-Debye behavior has been often reported in Fe-based superconductors and ascribed to a large Einstein contribution or a low Debye temperature T_D . Because an Einstein phonon contribution is negligible below 25 K in LiFeAs, a second term of the harmonic-lattice approximation is added to improve the Debye phonon specific heat as in Ref. 23: $C_n = \gamma_n(0)T + \beta_1 T^3 + \beta_2 T^5$. The specific heat is best described by the least-squares fit with $\gamma_n(0) = 17.0 \pm 0.9 \text{ mJ/mol K}^2$, $\beta_1 = 0.231 \pm 0.004 \text{ mJ/mol K}^4$, and $\beta_2 \simeq -0.0001 \text{ mJ/mol K}^6$. The electronic Sommerfeld coefficient $\gamma_n(0) (=17.0 \pm 0.9 \text{ mJ/mol K}^2)$ at zero magnetic field in the normal state is comparable with previously reported values of 20, 10, and 23 mJ/mol K^2 from Refs. 22, 23 and 25, respectively. The Debye temperature estimated from the fit is 294 K, which is similar to 310 K from Ref. 23. Figure 1(b) shows the electronic entropy in the normal (squares) and superconducting (circles) states after subtracting the nonelectronic contribution. The two entropies become equal at T_c , which satisfies the entropy constraint $0 = \int_0^{T_c} (C - C_n)/T dT$. From the electronic entropy in Fig. 1(b), we estimate the superconducting condensation energy $U = \int_0^{T_c} (S_{en} - S_{es})dT = B_c(0)^2/2\mu_0 \simeq 363 \text{ mJ/mol}$ and thermodynamic critical field $B_c(0) \simeq 0.23 \text{ T}$. When we use the Ginzburg-Landau parameter $\kappa = \lambda_{ab}/\xi_{ab} = 29 \pm 7$ of LiFeAs from a small-angle neutron scattering (SANS) experiment,¹⁴ the upper critical field $\mu_0 H_{c2}^{\parallel c} [= \sqrt{2}\kappa B_c(0)]$

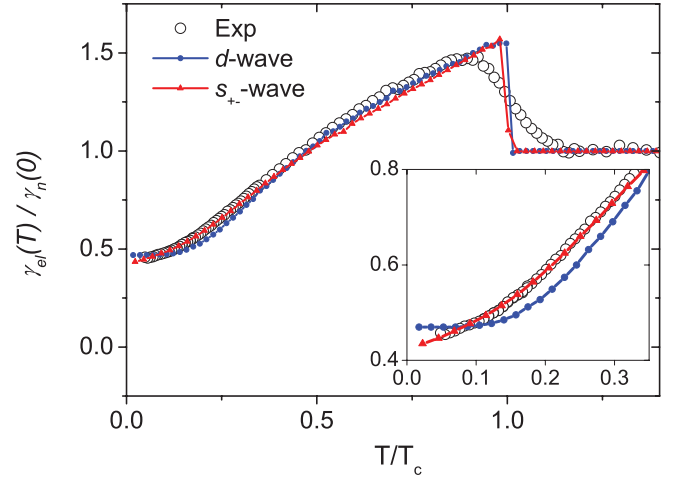


FIG. 2. (Color online) Normalized electronic specific heat coefficient (black open circles) and the best fits of the two SC gap models: d -wave (blue circles) and s_{\pm} -wave (red triangles) models. For the d -wave model, $2\Delta_{\max}/T_c = 3.5$ and $\Gamma = n_{\text{imp}}/\pi N_{\text{normal}} = 0.13$ are obtained for the best results. Here, Δ_{\max} is the maximum gap of the d -wave gap $\Delta(\theta)$. For the s_{\pm} -wave model, $|\Delta|_{\text{small}}/|\Delta|_{\text{large}} = 0.46$, $2\Delta_{\text{large}}/T_c = 3.8$, and $\Gamma = n_{\text{imp}}/\pi N_{\text{total}} = 0.17$ are obtained from the least-squares fit. We note that the inversely related ratios between $|\Delta|_{\text{small}}/|\Delta|_{\text{large}}$ and $N_{\text{small}}/N_{\text{large}}$ are an intrinsic property of the s_{\pm} -wave pairing model with a dominant interband pairing interaction (Ref. 27). Inset: Low-temperature specific heat in the main panel is magnified to show a notable difference between the two gap models.

is $9.4 \pm 2.3 \text{ T}$. For comparison, $\mu_0 H_{c2}^{\parallel c}$ from penetration measurements is 17 T.²⁶

Figure 2 shows the electronic specific heat coefficient of LiFeAs at zero magnetic field after subtracting the phononic contribution: $\gamma_{el}(T) = C_{el}/T = (C - C_{ph})/T$. The specific heat jump ΔC at T_c is 7.65 mJ/mol K^2 at zero field. The jump relative to the normal state specific heat C_n is $0.5 (= \Delta C/C_n)$, which is much smaller than the BCS value 1.43, indicating that the quasiparticles participating in the SC condensation experience strong elastic scattering because inelastic scattering usually enhances the jump ratio.²⁸ We note that the small value of the jump could be partially due to the multiband nature of superconductivity in LiFeAs.²⁹ The substantial value of the Sommerfeld coefficient γ_0 in the SC state, which accounts for about 45% of the normal state value $\gamma_n(0)$, also supports the presence of strong (unitary) scatterers because weak (Born limit) scatterers are not capable of inducing states inside the SC gap of unconventional superconductors.²⁷ These results suggest that any model to explain the nature of the SC gap symmetry of LiFeAs should take into account the effects of impurity scattering.

To extract information on the gap symmetry from the specific heat of LiFeAs, we consider two typical unconventional SC gap models that represent two extreme limits, i.e., a d -wave SC gap with nodes and a s_{\pm} -wave gap without nodes, and fit the experimental data in Fig. 2. Here we used the d -wave model to represent the generic behavior of a nodal SC gap state. The impurity effect is calculated using the self-consistent T -matrix approximation (SCTA).²⁷ In each gap model, we determine the fitting parameters such as $2\Delta/T_c$, the impurity

concentration parameter $\Gamma = n_{\text{imp}}/\pi N(0)$ by finding the best overall fit to the data, where $N(0)$ is the zero-energy density of states. The results are shown in Fig. 2 overlaid with the experimental data. Both models provided reasonably good fittings for the overall shape, the specific heat jump ΔC , and the $\gamma_{\text{el}}(T = 0 \text{ K})$ value. However, we find that the two models show qualitative differences for $\gamma_{\text{el}}(T)$ at low temperatures and this low-temperature behavior of $\gamma_{\text{el}}(T)$ is what reflects the intrinsic properties of the gap symmetry, with which we can unambiguously identify the most compatible gap symmetry.

A pure d -wave superconductor is expected to produce a T -linear specific heat coefficient such as $\gamma(T) = \alpha T$ because of the V -shaped density of state (DOS) $N(\omega) \sim \alpha' \omega$. However, the large value of $\gamma(T = 0)$ ($\sim 0.45\gamma_n$) indicates a substantial amount of unitary impurities. When the unitary impurities create a zero-energy impurity band inside the d -wave gap, the DOS around zero energy becomes a constant, $N(\omega) \sim N_0$, which in turn produces a constant, temperature-independent, specific heat coefficient $\gamma(T)$ for a finite range of low temperatures, as can be seen in the inset of Fig. 2 (blue circles). Our experimental data, however, show $\gamma(T) \sim \gamma_0 + \alpha T$, implying that the low energy DOS should have the form

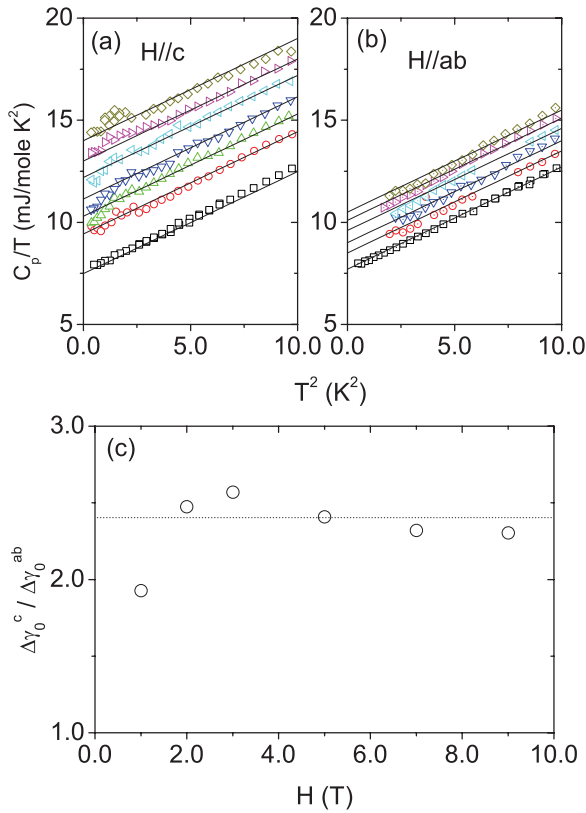


FIG. 3. (Color online) Low-temperature specific heat capacity for magnetic fields applied parallel to the crystalline c axis and ab plane in (a) and (b), respectively. In (a) the magnetic field intensity is 0, 1, 2, 3, 5, 7, and 9 T from bottom to top curves, and it is 0, 1, 3, 5, 7, and 9 T in (b). Straight lines are the results from the least-squares fit of $C/T = \gamma(H) + AT^2$ and used to obtain the zero temperature value of C/T . (c) Anisotropy of the Sommerfeld coefficient which is obtained from the extrapolation of the data in (a) and (b) for the two field orientations. Here $\Delta\gamma_0^c = \gamma_0^c(H) - \gamma_0^c(0T)$ for magnetic field along the c axis.

$N(\omega) \sim N_0 + \alpha' \omega$. This type of constant+ V -shaped DOS was indeed predicted for an s_{\pm} -wave gap with unitary impurities.²⁷ As can be seen in Fig. 2 and its inset, the s_{\pm} -wave gap model with unitary impurities provides an excellent fit at low temperatures as well as for the overall shape of $\gamma_{\text{el}}(T)$, but the d -wave model fails to explain the low-temperature behavior.

The dependence on magnetic field of the low-temperature specific heat of LiFeAs is shown in Figs. 3(a) and 3(b) for different field orientations of $H \parallel c$ and $H \perp c$, respectively. The lack of a Schottky-like anomaly up to the highest applied magnetic field enables us to unambiguously determine the Sommerfeld coefficient $\gamma(H)$ from the least-squares fits of $C(H)/T = \gamma(H) + AT^2$ to the low- T specific heat. As shown in Fig. 3(c), the anisotropy in the quasiparticle density of states $[\gamma_0^c(H) - \gamma_0]/[\gamma_0^{ab}(H) - \gamma_0]$ is almost constant (≈ 2.4) over the experimental field range and an anisotropy ratio of the upper critical fields between the two field directions is estimated to be 1.7 ± 0.2 through the relationship^{24,30} $\delta\gamma_0^c/\delta\gamma_0^{ab} = (0.5/0.3)(H_{c2}^{ab}/H_{c2}^c)^{0.7}$. The H_{c2} anisotropy from this thermodynamic measurement is in good agreement with that obtained from transport properties where H_{c2} was directly measured under high magnetic field.^{26,31}

A sublinear magnetic field dependence of $\gamma_0(H)$ is displayed in Fig. 4, which is often taken as evidence for a nodal gap structure such as a d -wave state that is known to have a generic \sqrt{H} dependence due to Doppler effects of the nodal quasiparticles by the supercurrent circulating around the vortices. Recent theoretical work, however, showed that the s_{\pm} -wave state with different gap sizes ($\Delta_{\text{small}} \neq \Delta_{\text{large}}$) can also show a strong field dependence of $\gamma(H) \propto \sqrt{H} - H$.³² In Fig. 4, we show theoretical calculations for both s_{\pm} -wave (dotted line) and d -wave (dashed line) models to fit the $\gamma_0(H)$ data with $H \parallel c$, where we use the same fitting parameters

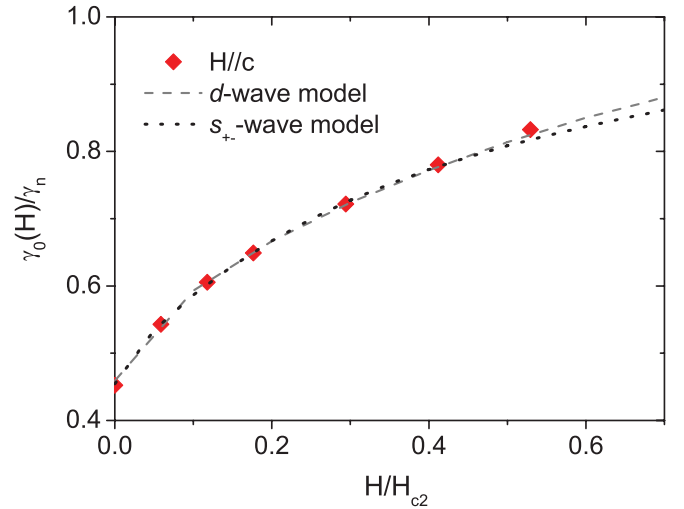


FIG. 4. (Color online) Field-dependent Sommerfeld coefficient extrapolated from Fig. 3(a) for field applied along the crystalline c axis. The black dotted line is the theoretical fit with the s_{\pm} -wave model and the gray dashed line is the fit with the d -wave model, respectively. Here we used the upper critical field H_{c2} of 17 T from Ref. 26. The error bars of the γ values are less than the size of the symbols.

obtained from the analysis of the specific heat as a function of temperature (see Fig. 2). It is clear that the s_{\pm} -wave model equally well reproduces the field dependence of $\gamma(H)$ which has been taken as a signature for a nodal gap structure. Thus, in combination with our analysis of the zero-field temperature dependence, our data favors the sign changing multiband superconductivity of the s_{\pm} -wave state.

To summarize, we have reported the specific heat capacity of a LiFeAs single crystal under magnetic field. The small specific heat jump ratio at T_c and substantial residual density of states at $T = 0$ K in the SC state indicate that impurity effects due to strong unitary scatterers should be included to explain the specific heat results. The zero-field specific heat data at high temperatures above 2 K and sublinear magnetic field dependence of the Sommerfeld coefficient are equally

well described by nodal and nodeless multiband SC gaps with impurity effects. However, the low-temperature electronic specific heat below 2 K excludes the nodal d -wave state, but is consistent with the sign changing multiband superconductivity of the s_{\pm} -wave state.

This work was supported by NRF grants (No. 2010-0029136, No. 2011-0021645, and No. 2010-0007487) funded by the Korea government (MEST). Work at Los Alamos was performed under the auspices of the US Department of Energy/Office of Science and supported in part by the Los Alamos LDRD program. Y.B. was supported by Grant No. NRF-2010-0009523 funded by the National Research Foundation of Korea. D.J. acknowledges support from the Postdoctoral Research Program of Sungkyunkwan University.

*tp8701@skku.edu

†ykbang@chonnam.co.kr

¹Y. Kamihara, H. Hiramatsu, M. Hirano, R. Kawamura, H. Yanagi, T. Kamiya, and H. Hosono, *J. Am. Chem. Soc.* **130**, 3296 (2008).

²K. Ishida, Y. Nakai, and H. Hosono, *J. Phys. Soc. Jpn.* **78**, 062001 (2009).

³G. R. Stewart, *Rev. Mod. Phys.* **83**, 1589 (2011).

⁴P. J. Hirschfeld, M. M. Korshunov, and I. I. Mazin, *Rep. Prog. Phys.* **74**, 124508 (2011).

⁵A. F. Kemper, T. A. Maier, S. Graser, H.-P. Cheng, P. J. Hirschfeld, and D. J. Scalapino, *New J. Phys.* **12**, 073030 (2010).

⁶K. Kuroki, H. Usui, S. Onari, R. Arita, and H. Aoki, *Phys. Rev. B* **79**, 224511 (2009).

⁷E. van Heumen, J. Vuorinen, K. Koepf, F. Massee, Y. Huang, M. Shi, J. Klei, J. Goedkoop, M. Lindroos, J. van den Brink, and M. S. Golden, *Phys. Rev. Lett.* **106**, 027002 (2011).

⁸Y.-J. Song, J. S. Ghim, B. H. N. Min, Y. S. Kwon, M. H. Jung, and J.-S. Rhyee, *Appl. Phys. Lett.* **96**, 212508 (2010).

⁹M. J. Pitcher, D. R. Parker, P. Adamson, S. J. C. Herkelrath, A. T. Boothroyd, R. M. Ibberson, M. Brunelli, and S. J. Clarke, *Chem. Commun.* **2008**, 5918 (2008).

¹⁰X. C. Wang, Q. Q. Liu, Y. X. Lv, W. B. Gao, L. X. Yang, R. C. Yu, F. Y. Li, and C. Q. Jin, *Solid State Commun.* **148**, 538 (2008).

¹¹J. H. Tapp, Z. Tang, B. Lv, K. Sasmal, B. Lorenz, Paul C. W. Chu, and A. M. Guloy, *Phys. Rev. B* **78**, 060505(R) (2008).

¹²J. S. Kim, E. G. Kim, and G. R. Stewart, *J. Phys.: Condens. Matter* **21**, 252201 (2009).

¹³K. Gofryk, A. S. Sefat, E. D. Bauer, M. A. McGuire, B. C. Sales, D. Mandrus, J. D. Thompson, and F. Ronning, *New J. Phys.* **12**, 023006 (2010).

¹⁴D. S. Inosov, J. S. White, D. V. Evtushinsky, I. V. Morozov, A. Cameron, U. Stockert, V. B. Zabolotnyy, T. K. Kim, A. A. Kordyuk, S. V. Borisenko, E. M. Forgan, R. Klingeler, J. T. Park, S. Wurmehl, A. N. Vasiliev, G. Behr, C. D. Dewhurst, and V. Hinkov, *Phys. Rev. Lett.* **104**, 187001 (2010).

¹⁵H. Kim, M. A. Tanatar, Y. J. Song, Y. S. Kwon, and R. Prozorov, *Phys. Rev. B* **83**, 100502(R) (2011).

¹⁶M. A. Tanatar, J. P. Reid, S. Rene de Cotret, N. Doiron-Leyraud, F. Laliberte, E. Hassinger, J. Chang, H. Kim, K. Cho, Y. J. Song,

Y. S. Kwon, R. Prozorov, and L. Taillefer, *Phys. Rev. B* **84**, 054507 (2011).

¹⁷Y. Imai, H. Takahashi, K. Kitagawa, K. Matsubayashi, N. Nakai, Y. Nagai, Y. Uwatoko, M. Machida, and A. Maeda, *J. Phys. Soc. Jpn.* **80**, 013704 (2011).

¹⁸Z. Li, Y. Ooe, X.-C. Wang, Q.-Q. Liu, C.-Q. Jin, M. Ichioka, and G.-Q. Zheng, *J. Phys. Soc. Jpn.* **79**, 083702 (2010).

¹⁹K. Sasmal, B. Lv, Z. Tang, F. Y. Wei, Y. Y. Xue, A. M. Guloy, and C. W. Chu, *Phys. Rev. B* **81**, 144512 (2010).

²⁰K. Umezawa, Y. Li, H. Miao, K. Nakayama, Z.-H. Liu, P. Richard, T. Sato, J. B. He, D.-M. Wang, G. F. Chen, H. Ding, T. Takahashi, and S.-C. Wang, *Phys. Rev. Lett.* **108**, 037002 (2012).

²¹C. Platt, R. Thomale, and W. Hanke, *Phys. Rev. B* **84**, 235121 (2011).

²²F. Wei, F. Chen, K. Sasmal, B. Lv, Z. J. Tang, Y. Y. Xue, A. M. Guloy, and C. W. Chu, *Phys. Rev. B* **81**, 134527 (2010).

²³U. Stockert, M. Abdel-Hafiez, D. V. Evtushinsky, V. B. Zabolotnyy, A. U. B. Wolter, S. Wurmehl, I. Morozov, R. Klingeler, S. V. Borisenko, and B. Buchner, *Phys. Rev. B* **83**, 224512 (2011).

²⁴D. J. Jang, A. B. Vorontsov, I. Vekhter, K. Gofryk, Z. Yang, S. Ju, J. B. Hong, J. H. Han, Y. S. Kwon, F. Ronning, J. D. Thompson, and T. Park, *New J. Phys.* **13**, 023036 (2011).

²⁵P. J. Baker, S. R. Giblin, F. L. Pratt, R. H. Liu, G. Wu, X. H. Chen, M. J. Pitcher, D. R. Parker, S. J. Clarke, and S. J. Blundell, *New J. Phys.* **11**, 025010 (2009).

²⁶K. Cho, H. Kim, M. A. Tanatar, Y. J. Song, Y. S. Kwon, W. A. Coniglio, C. C. Agosta, A. Gurevich, and R. Prozorov, *Phys. Rev. B* **83**, 060502(R) (2011).

²⁷Y. Bang, H.-Y. Choi, and H. Won, *Phys. Rev. B* **79**, 054529 (2009).

²⁸Y. Bang and A. V. Balatsky, *Phys. Rev. B* **69**, 212504 (2004).

²⁹F. Bouquet, R. A. Fisher, N. E. Phillips, D. G. Hinks, and J. D. Jorgensen, *Phys. Rev. Lett.* **87**, 047001 (2001).

³⁰M. Ichioka, A. Hasegawa, and K. Machida, *Phys. Rev. B* **59**, 184 (1999).

³¹S. Khim, B. Lee, J.-W. Kim, E.-S. Choi, G. R. Stewart, and K.-H. Kim, *Phys. Rev. B* **84**, 104502 (2011).

³²Y. Bang, *Phys. Rev. Lett.* **104**, 217001 (2010).